ACS OMEGA

http://pubs.acs.org/journal/acsodf

Article

Bitumen Recovery Performance of SAGD and Butane- and Hexane-Aided SAGD in the Presence of Shale Barriers

Ashish Kumar and Hassan Hassanzadeh*

Cite This: *ACS Omega* 2022, 7, 20280−20290

Read Online

ACCESS | Metrics & More | Article Recommendations

ABSTRACT: Oil and gas formations are commonly found to be heterogeneous, and one of the most common occurrences of reservoir heterogeneity is the presence of shale barriers. Shale barriers typically have very low permeability and high initial water saturation. Due to low permeability, these barriers obstruct the oil drainage path, specifically in thermal recovery methods such as steam-assisted gravity drainage (SAGD). In addition to flow assistance, they also lead to heat losses due to absorption by the high initial water saturation. Expanding solvent steam-assisted gravity drainage (ES-SAGD) is a hybrid technique comprising solvent co-injection along with steam. Solvent being in the vapor phase can potentially overcome the restricted path due to the presence of shale barriers. This paper presents a numerical simulation study on comparison between SAGD and ES-SAGD in the presence of shale barriers. SAGD and ES-SAGD with hexane and butane are numerically simulated for 240 lognormally generated shale realizations. First, both recovery processes are analyzed over the whole simulation period. Additionally, they have also been evaluated at multiple cumulative steam oil ratio cut-offs at 2, 2.5, 3, and 3.5. Transition points are defined and explained to cluster the shale density/fractions based on similar behaviors. It was shown that the oil that cannot be mobilized and produced by SAGD because shale barriers can be reached by the vaporized solvent through tortuous paths and recovered. Also, thermal losses are reduced because of lower steam chamber temperature. This led to efficient results for ES-SAGD over SAGD in heterogeneous formations.

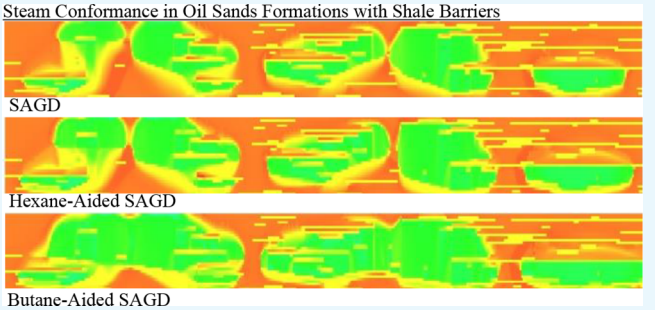

1. INTRODUCTION

The energy demand is continuously on the rise throughout the world. Fossil fuels are one of the major sources of energy for the foreseeable future. According to the BP Statistical Review of World Energy 2020, nearly 84% of total energy consumption in the world comes from fossil fuels. Among fossil fuels, oil and natural gas share is 67%. While conventional oil and gas reservoirs still provide the major fraction of production, heavy oil reservoirs become a vital resource to produce oil and gas during the last few decades. Heavy oil generally has a low API of less than 20°.[1] Extra-heavy oil is another type of heavy oil where API is less than 10° and viscosity is more than 10,000 cP. Most extra-heavy oil reservoirs are present in Canada and Venezuela. In Canada, these extra-heavy oil reservoirs are commonly called bitumen or oil sands. According to the Natural Resource Canada (NRC), Canada, has ∼170 billion barrels of proven reserves, and 96% of the total are present in the form of bitumen. Over time, bitumen extraction has evolved significantly, leading to efficient production with lesser carbon footprints. In recent times, as the world is becoming more vocal about reducing carbon emissions, oil sands industries have shown tremendous potential to further reduce their emissions toward the goal of net-zero carbon production.

In the early days, bitumen was produced mainly by mining. After the evolution of thermal recovery methods based on steam injection, oil sand production has increased significantly. Among these methods, steam-assisted gravity drainage (SAGD) is one of the most successful recovery processes for bitumen extraction introduced by the late Roger Butler (1927−2005) in the 1970s. SAGD is a gravity-based thermal recovery method that consists of well pairs drilled horizontally, one above the other; the lower wellbore is the producer, whereas the upper acts as an injector. Steam is injected continuously through the injector, which creates an expanding steam chamber heating the cold bitumen and subsequently flowing toward the producer due to gravity.[2] As bitumen extraction through mining was limited to very shallow deposits generally less than 75 m, SAGD revolutionized the oil sands production by targeting deeper formations that

Received: April 11, 2022
Accepted: May 25, 2022
Published: June 3, 2022

https://doi.org/10.1021/acsomega.2c02263
ACS Omega 2022, 7, 20280−20290

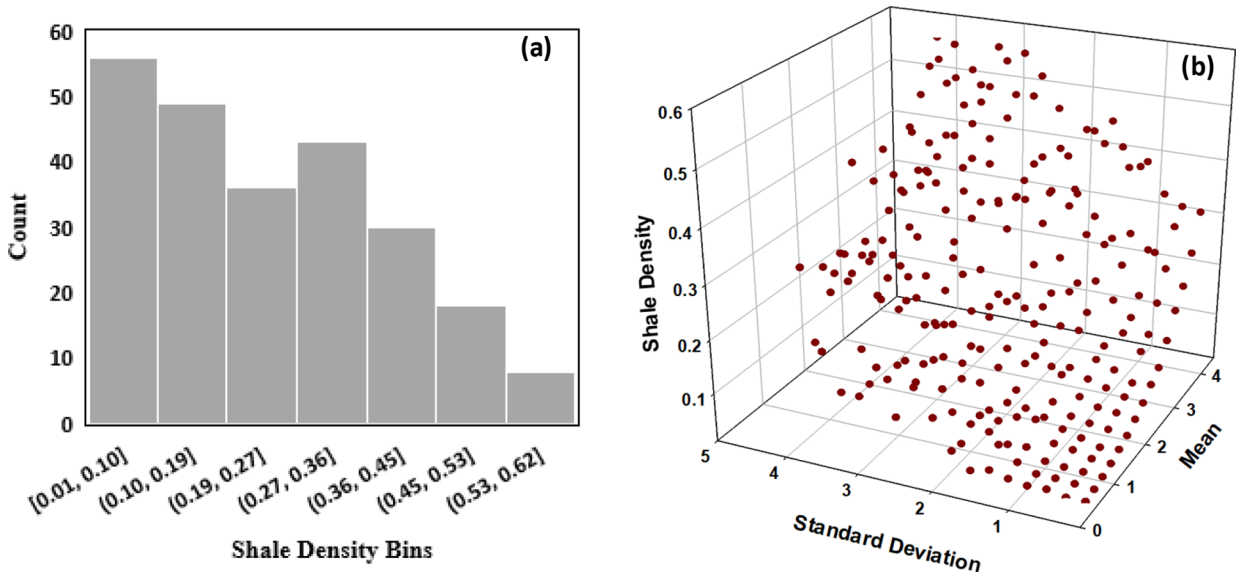

Figure 1. (a) Histogram for shale density (fraction) and (b) 3D scatter plot for shale density versus mean and standard deviation.

could not be possible using open-pit mining. SAGD is an energy-intensive process, and hence continuous research on reducing emissions while also increasing efficiency is ongoing. As a result, Nasr et al. introduced expanding solvent SAGD (ES-SAGD).[3] During this process, a hydrocarbon solvent is co-injected along with the steam. According to Nasr et al., solvents that have close to or similar condensation properties as steam are most efficient to be co-injected with steam.[3] There were two main reasons behind the use of solvents, first to have an additional reduction of bitumen viscosity due to the dilution effect of solvent and second, less energy requirement in the form of steam.[3] Numerous studies have been performed for the selection of efficient solvents for ES-SAGD. According to Nasr et al., hexane and heptane were considered as good candidates for ES-SAGD.[3] Some studies have also reported better performance of higher carbon number solvents.[4,5] Khaledi et al. studied ES-SAGD operating conditions along with solvent/bitumen/water phase interaction properties to show their impact on the solvent co-injection process.[6] They observed that the boiling range of solvent influences the solvent condensation along with the steam chamber during the process. They also inferred that the composition of solvents could be engineered to improve the efficiency of the ES-SAGD process. In another study, Sabet et al. demonstrated that solvents with a carbon number from 7 to 9 lead to convective dissolution that could improve bitumen dilution by solvent.[7] Nourozieh et al. conducted experiments over a wide range of temperatures and pressures to study the phase behavior of pentane and Athabasca bitumen.[8] They reported a significant reduction in bitumen viscosity with the help of pentane dissolution at experimental pressure and temperature conditions. Zirrahi et al. also carried out experiments to obtain thermophysical property data for various solvents from methane to pentane.[9] They reported that lighter solvents were more efficient in viscosity reduction at low-temperature conditions, and at higher temperatures, heavier solvents tend to perform better. The solvent selection and its injected concentration in an ES-SAGD process are still challenging and require a careful study of phase interaction between solvent and reservoir fluids. Various pilot projects were executed, which have shown promising results using solvent co-injection.[10] The main aim of this paper is to evaluate the performance of SAGD and ES-SAGD and compare them further in the presence of distributed shale barriers. Shale barriers obstruct the bitumen drainage path along with excessive heat loss due to their high-water saturation. Various studies have been done to demonstrate the impact of shale barriers on SAGD performance.[11−24] Kumar and Hassanzadeh have presented a detailed literature review on the impact of shale barriers on SAGD and ES-SAGD.[25] However, very few studies are available regarding the impact of shales on ES-SAGD performance.[26−29] A major industry standard to assess the performance of SAGD and ES-SAGD is the steam oil ratio (SOR). The conventional range of the SOR for an efficient SAGD process in a homogeneous reservoir tends to fall between 2 and 3. Studies based on ES-SAGD performance evaluation in the presence of shale barriers were based on the use of heptane and hexane as solvents.[26,28] All the studies reported an improved performance by ES-SAGD over SAGD in the presence of shale barriers. This paper proposes a further detailed study on comparing SAGD and ES-SAGD in heterogeneous reservoirs over a wide range of shale densities. A total of 240 different shale realizations are prepared using log-normal distribution to cover a wide range of heterogeneity, where shale density spreads over 0.01 to 0.6. Butane (a lighter solvent) and hexane (a comparatively heavier solvent) are used to study the behavior of ES-SAGD. An optimized concentration of approximately 18% volumetric fraction injection is used in this study. Initially, both SAGD and ES-SAGD are compared over the whole simulation period (∼ 20 years). Later economic cut-offs of the cumulative SOR (cSOR) (i.e., 2, 2.5, 3, and 3.5) are imposed to analyze the data and extract the results.

2. RESERVOIR MODEL

A 2D reservoir model is constructed to analyze the impact of shale barriers on SAGD and ES-SAGD performance. This model comprises 375 × 30 grid blocks in *x*- and *z*-directions with a grid size of 1 meter, which is common in thermal reservoir simulation. There were five well pairs present inside the model, having a length of 1 km each in the *y*-direction. The reservoir thickness is 30 m, and the producer is 1 m from the bottom of the reservoir, while the injector is located 5 m above the producer. Shale realizations are generated by using a log-

https://doi.org/10.1021/acsomega.2c02263
ACS Omega 2022, 7, 20280−20290

normal distribution. A single shale barrier is characterized by location coordinates (x,z) and length (L_s). A typical shale realization for a given σ and μ is generated based on locations of shale barriers (x_i, z_i) obtained using a uniform distribution, shale barrier length distribution (L_{si}) based on the log-normal distribution, and the given sample size or the number of shale barriers (N_s), where x is the random variable, μ is the mean of the log of the distribution, and σ is the standard deviation of the log of the distribution. The thickness for all shale barriers is kept constant as 1 m. This procedure for the generation of shale barrier realization has been previously reported.[30] The mean of the distribution is varied from 0.5 to 4, and the standard deviation is varied from 0.25 to 4 with a step size of 0.25 for each, which is shown in Figure 1b. Shale density is defined as the fraction representing volume of shale divided by total reservoir volume. Figure 1a represents a histogram for shale density bins with their respective count used in the simulation studies. Shale density is used as a measure of heterogeneity to analyze the simulation results in the upcoming sections. A total of 240 realizations were prepared where the mean of shale density was 0.236 and median was 0.215. Other important descriptive statistics include minimum shale density of 0.011, maximum shale density of 0.601, and the standard deviation of 0.153. Kumar and Hassanzadeh presented a detailed workflow for generating the shale heterogeneity for this study.[30] Porosity and permeability of clean sand are taken as 0.3 and 5000 mD, respectively, as generic values for oilsand formations.

Shale barriers' porosity and permeability values are considered to be 0.05 and 10 mD, respectively. Connate water saturation for clean sand and shales are assumed as 0.15 and 0.4, respectively. Shale barrier thickness is 1 m and was kept constant for all the shale realizations. Stone's second model is used for calculating two-phase relative permeability values, and capillary pressure and asphaltene precipitation are assumed to be negligible. We assumed steam injection at an injector with 100% steam quality at 242.6 °C with a maximum water injection rate of 600 m^3/day per well. A 6-month preheating period has been carried out for each simulation study. All these 240 heterogeneous models are subjected to numerical simulation over 20 years using CMG STARS.[31]

Three components, including water, solution gas, and bitumen, are used for SAGD simulations. For ES-SAGD simulations, four components, including water, solution gas, bitumen, and solvent (C_4 or C_6), are used. All thermophysical properties are obtained based on the previously reported experimental data.[30,32,33] All the 240 shale realization cases are subjected to simulation for three different scenarios: the first scenario is normal SAGD, the second scenario is ES-SAGD with C6 co-injection, and the third one is ES-SAGD with C4 co-injection. Therefore, this study is based on data derived from 720 cases of reservoir simulations. Solvent and bitumen production is derived separately as different production streams. All the results are presented in the form of descriptive statistics of the simulation results. Figure 2 represents a sample reservoir model with distributed shales for a given mean and standard deviation.

3. RESULT AND DISCUSSION

3.1. Comparison of SAGD and ES-SAGD over the Complete Simulation Period of 20 Years. We start with the major performance criteria such as Bitumen Recovery (%) and the cSOR comparison between these processes. Out of 240 total shale realizations results, a total of 216 different shale realizations cases have been selected to discard outliers present in the simulation data. Figure 3 presents a holistic view of steam conformance in a given heterogeneous reservoir for SAGD, C6 ES-SAGD, and C4 ES-SAGD after 3 years during the simulation period.

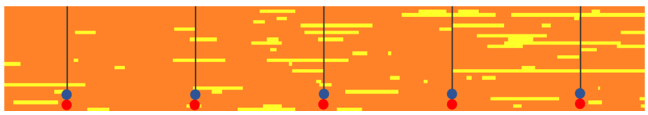

Figure 2. 2D $(x-z)$ view of permeability field with mean 2.5 and standard deviation 1. Red and blue markers show the location of production and injection wells, respectively.

We observed better steam-solvent chamber expansion for C4 ES-SAGD as compared to C6 ES-SAGD. C4 has delayed condensation relative to C6, which led to better propagation of C4 vapor through the shale heterogeneity and hence efficient steam conformance. This phenomenon will be explained and validated with the simulation data in the upcoming sections. Figure 4 shows the simulation results for both SAGD and ES-SAGD processes over the whole simulation period of 20 years. We observe a common trend in both the processes where recovery is decreasing with the increase in shale density and cSOR is increasing. The main reason is the increase in reservoir heterogeneity due to higher shale fractions. We also observed that the rate of decrease in the recovery factor and the increase in cSOR are not constant but have two distinct trends. We can term the point as a transition point on the shale density scale to separate these trends based on the rate of increase/decrease in recovery or cSOR. In other words, the transition point can be defined as the shale density at which the rate of increase/decrease in the key performance measure varies significantly. Hence, we further evaluated and divided the shale density into two parts, one with shale density less or equal to 0.2 and the other more than 0.2, which will be called LSHD and HSHD, respectively, for the analysis in later sections. The transition in recovery and cSOR trends for C4 ES-SAGD occurs at a higher shale density than C6 ES-SAGD, whereas the transition point for C6 ES-SAGD is higher than SAGD. The three dotted lines in Figure 4a point to different values for transition points for SAGD, C6 ES-SAGD, and C4 ES-SAGD, respectively. This shows that ES-SAGD is able to improve recovery in higher shale fractions relative to SAGD.

Figure 5 shows the variation of recovery (%) and cSOR within shale density $\leq$0.2 and >0.2. As explained previously, we denote shale density $\leq$0.2 as LSHD and >0.2 as HSHD. The rate of decline in recovery factor for both SAGD and ES-SAGD is steeper in HSHD relative to LSHD; a similar behavior can be seen in the rate of increase in cSOR. We also noticed that the difference between recovery factors and cSOR between SAGD and ES-SAGD is more distinct in HSHD relative to LSHD. As with increasing shale density, an increase in the recovery factor due to ES-SAGD is more pronounced in HSHD relative to LSHD. In LSHD, the means of recovery for SAGD, C6 ES-SAGD, and C4 ES-SAGD are 85.52, 90.11, and 89.97, respectively, while the means of the cSOR values are 4.22, 3.98, and 3.77, respectively. The standard deviations of recovery for SAGD, C6 ES-SAGD, and C4 ES-SAGD are 10.86, 9.3, and 7.6, and those of the cSOR values are 0.76, 0.46, and 0.27, respectively. In HSHD, the means of recovery for SAGD, C6 ES-SAGD, and C4 ES-SAGD are 47.76, 57.02, and 61.81, respectively, while the means of the cSOR values are 8.53, 6.88, and 5.61, respectively. The standard deviation of recovery

https://doi.org/10.1021/acsomega.2c02263
ACS Omega 2022, 7, 20280−20290

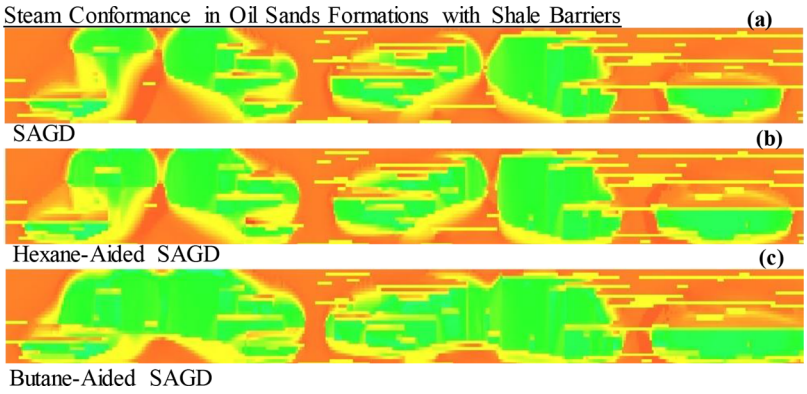

Figure 3. Steam conformance in oilsand formations with shale barriers after 3 years for (a) SAGD, (b) C6 ES-SAGD, and (c) C4 ES-SAGD.

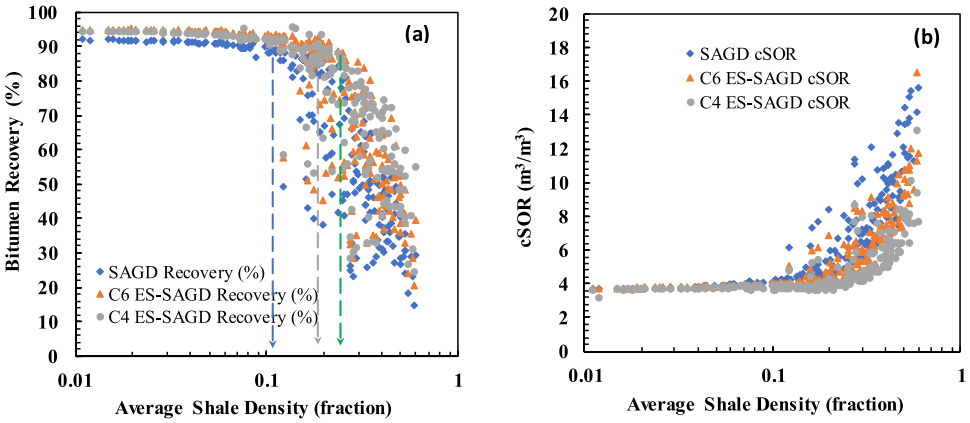

Figure 4. (a) Bitumen recovery (%) versus shale density and (b) cumulative SOR versus shale density.

for SAGD, C6 ES-SAGD, and C4 ES-SAGD are 16.88, 16.92, and 16.72, and those of the cSOR values are 3.02, 2.13, and 1.64, respectively. The standard deviation in HSHD is significantly higher than in LSHD due to higher shale fractions. We observed that ES-SAGD with C4 has somewhat performed better than ES-SAGD with C6 in the presence of shale barriers in the HSHD case and almost similar in the LSHD case over the whole simulation period. The reason can be due to the delayed or partial condensation of C4 in the presence of higher shale fractions, which allowed C4 to remain in vapor phase, enabling it to pass the tortuous paths of shale barriers and later mix with bitumen after condensation. Now, we look at the incremental percentage of recovery and solvent retention behavior ES-SAGD with C4 and C6.

The incremental percentage of recovery due to ES-SAGD and variation of solvent retention with the average shale density is shown in Figure 6a and Figure 6b, respectively. We observed that solvent retention tends to increase with higher shale density or heterogeneity. From the data, we saw that the average C6 retention is 23.57%, while the average C4 retention is 22.98%. Higher retention of C6 may be due to higher condensation temperature relative to C4. We have excluded any type of solvent blowdown normally done to recover the solvents retained after the production maturation. The average increase in recovery (%) for C6 ES-SAGD is 14.11%, and for C4 ES-SAGD, it is 20.44% over all shale realizations with a solvent injection volume fraction of 18%.

Analyzing the results over the total simulation period of 20 years cannot be a true representation of the system performance, as for an economical process, the cSOR is generally required to be less than 3. Hence, we have imposed different cSOR cut-offs of 2, 2.5, 3, and 3.5 for comparing both SAGD and ES-SAGD performance as per industry standards for a conclusive representation. The below sections will explain the results under each cut-off for the cSOR.

3.2. Cumulative SOR = 2. The first case is selected with a cSOR cut-off of 2. Simulation results are filtered and obtained where cSOR is either equal or less than 2 for both SAGD and ES-SAGD along with their timestamp. First, we will compare between SAGD and ES-SAGD and then later compare between C6 and C4 ES-SAGD. In Figure 7a, the times taken to reach a cSOR of 2 for both SAGD and ES-SAGD are plotted against shale density. Additionally, recovery (%) is also being plotted for both processes in Figure 7b. Solvent retention (%) and absolute recovery gain over SAGD for C6 and C4 ES-SAGD are shown in Figure 7c and Figure 7d, respectively.

Here, we focus on LSHD (shale density $\leq$ 0.2) and HSHD (shale density > 0.2), as explained in previous sections. From both Figure 6a,b, we observe a slanted L-shaped curve. From the results summarized in Table 1, we observe that both SAGD and ES-SAGD produce much better results in LSHD relative to HSHD. When comparing SAGD and ES-SAGD, we notice that the average absolute gain in recovery over SAGD is higher for C4 ES-SAGD relative to C6 ES-SAGD. Considering simulation results, ES-SAGD proves to be a better choice for LSHD. Extreme higher heterogeneity proves to be detrimental for both SAGD and ES-SAGD due to the presence of elongated continuous shale and higher shale fractions. We also observe that the average solvent retention is similar for C6 ES-SAGD for both LSHD and HSHD cases, whereas for C4 ES-SAGD, the

https://doi.org/10.1021/acsomega.2c02263
ACS Omega 2022, 7, 20280−20290

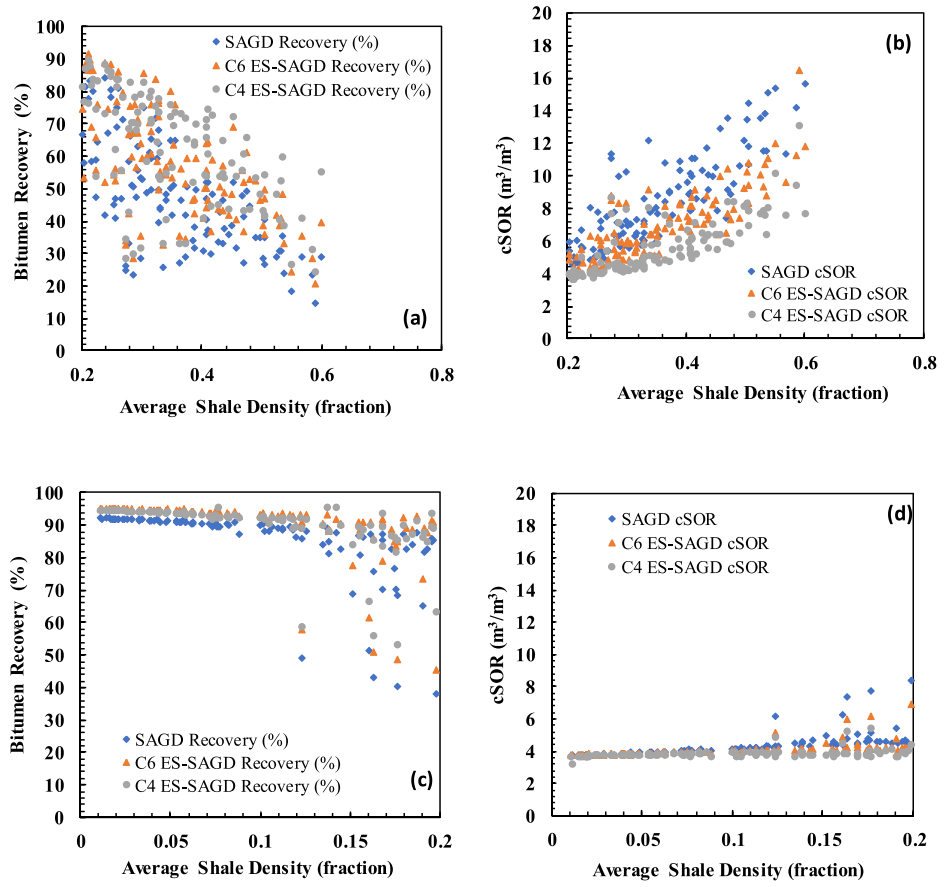

Figure 5. (a,b) Bitumen recovery (%) and cumulative SOR versus shale density (>0.2, HSHD) (c,d) bitumen recovery (%) and cumulative SOR versus shale density (≤0.2, LSHD).

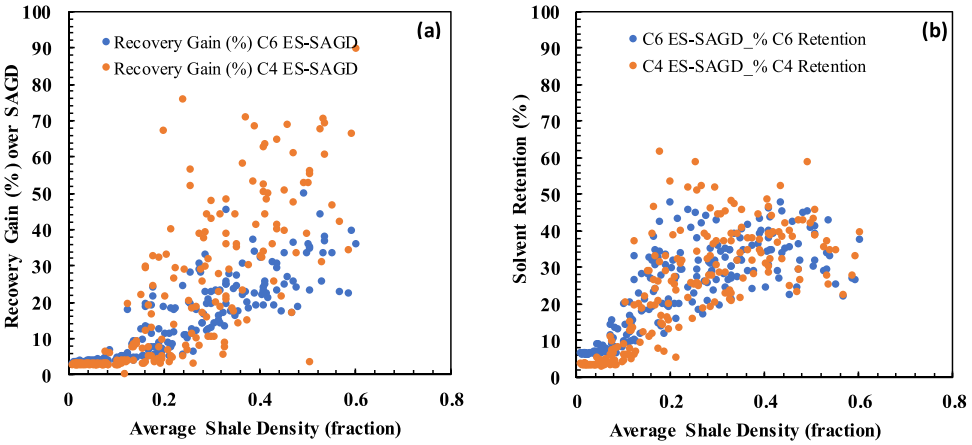

Figure 6. (a) Recovery gain (%) relative to SAGD and (b) solvent retention (%) for ES-SAGD.

average solvent retention is higher for HSHD relative to LSHD. Delayed condensation of C4 relative to C6 leads to better solvent transport in the vapor phase through the restricted paths in the presence of shales.

Using the analysis conducted over all heterogeneous shale realizations, we observed that under cSOR cut-off of 2, the transition point of average shale density is much lower than 0.2 and approximately equals 0.06. As noted, the transition point is when the rate of increase/decrease in the key performance measures is changing significantly, which can be seen in Figure 7a. We also observe the similar or almost equal transition point in each Figure 7a–d. We will see this transition point shifts rightward on the scale of the average shale density with the increase in cSOR cut-off.

3.3. Cumulative SOR = 2.5. Like the previous analysis, we analyzed the simulation results with a cSOR cut-off of 2.5. We observe that the transition point is shifted rightward on the average shale density scale. This transition point is still much lower than the transition point obtained for the total simulation period (i.e., shale density of 0.2).

Figure 8a,b presents the variation of simulation time and bitumen recovery versus average shale density for SAGD and ES-SAGD cases. Absolute/net gain of recovery over SAGD and solvent retention for ES-SAGD cases are depicted in Figure 8c,d,

https://doi.org/10.1021/acsomega.2c02263
ACS Omega 2022, 7, 20280−20290

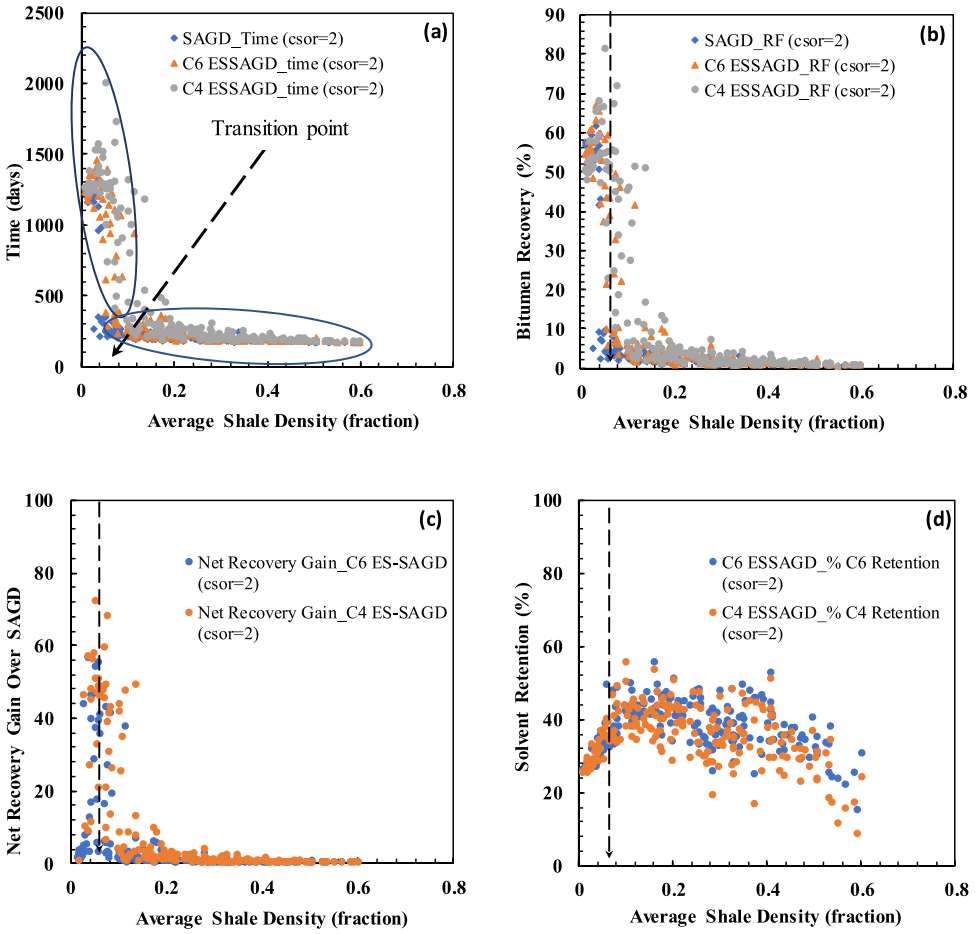

Figure 7. (a) Simulation time for cSOR = 2, (b) recovery (%) for cSOR = 2, (c) absolute recovery gain relative to SAGD for cSOR = 2, and (d) solvent retention (%) for cSOR = 2.

Table 1. Average of Simulation Results at cSOR = 2

	simulation time to reach cSOR = 2 (days)		bitumen recovery (%)		solvent retention (%)			
case	LSHD	HSHD	LSHD	HSHD	LSHD	HSHD	net/absolute recovery gain (%)	transition point shale density
SAGD	446	182	14.7	1.2	NA	NA	NA	~0.06
C6 ES-SAGD	644	190	24.3	1.5	37.5	37.3	4.9	
C4 ES-SAGD	821	202	30.3	1.8	36.5	33.7	8.0	

respectively. From the plots, we observed that the transition point is approximately 0.12, which is higher than the transition point observed at a cSOR of 2 (Table 2).

Like previous observations, performance is better in LSHD compared to HSHD for both SAGD and ES-SAGD. The average bitumen recovery of C4 ES-SAGD is still less than 10% for both SAGD and ES-SAGD in the high-density shale range. In the case of solvent retention, both C4 and C6 ES-SAGD show a similar trend with lower retention in LSHD and higher in HSHD. In both LSHD and HSHD, solvent retention is lower for C4 ES-SAGD than C6 ES-SAGD. The average net gain in recovery for C6 ES-SAGD for cSOR = 2.5 is more than cSOR = 2, which is also similar for C4 ES-SAGD.

3.4. Cumulative SOR = 3. Here, we also analyze the results based on LSHD (shale density ≤ 0.2) and HSHD (shale density > 0.2), as explained in previous sections. Simulation times taken to reach a cSOR of 3 for both SAGD and ES-SAGD are against shale density are shown in Figure 9a. Recovery (%) is also shown for both processes in Figure 9b. Solvent retention (%) and absolute recovery gain over SAGD for C6 and C4 ES-SAGD are depicted in Figure 9c) and Figure 9d, respectively. The transition point denoted by the dotted line observed in Figure 9 is shifted rightward relative to lower cSOR cut-offs.

Table 3 presents the average values for simulation results for this case. We observed that at cSOR = 3, both SAGD and ES-SAGD can produce more than 50% of bitumen for the LSHD case. The average time taken by SAGD is around 7.96 years to reach this cSOR cut-off. In ES-SAGD, the average time taken by C4 ES-SAGD is 9.81 years, while C6 ES-SAGD took 11.75 years. We found that bitumen recovery for C4 ES-SAGD is close to 10% now for HSHD. Also, the average absolute gain in recovery for both C6 ES-SAGD and C4 ES-SAGD is higher relative to results obtained at cSOR = 2.5. We also observed that solvent retention decreases with the increase in cSOR cut-offs for both C4 ES-SAGD and C6 ES-SAGD in the LSHD case.

https://doi.org/10.1021/acsomega.2c02263
ACS Omega 2022, 7, 20280−20290

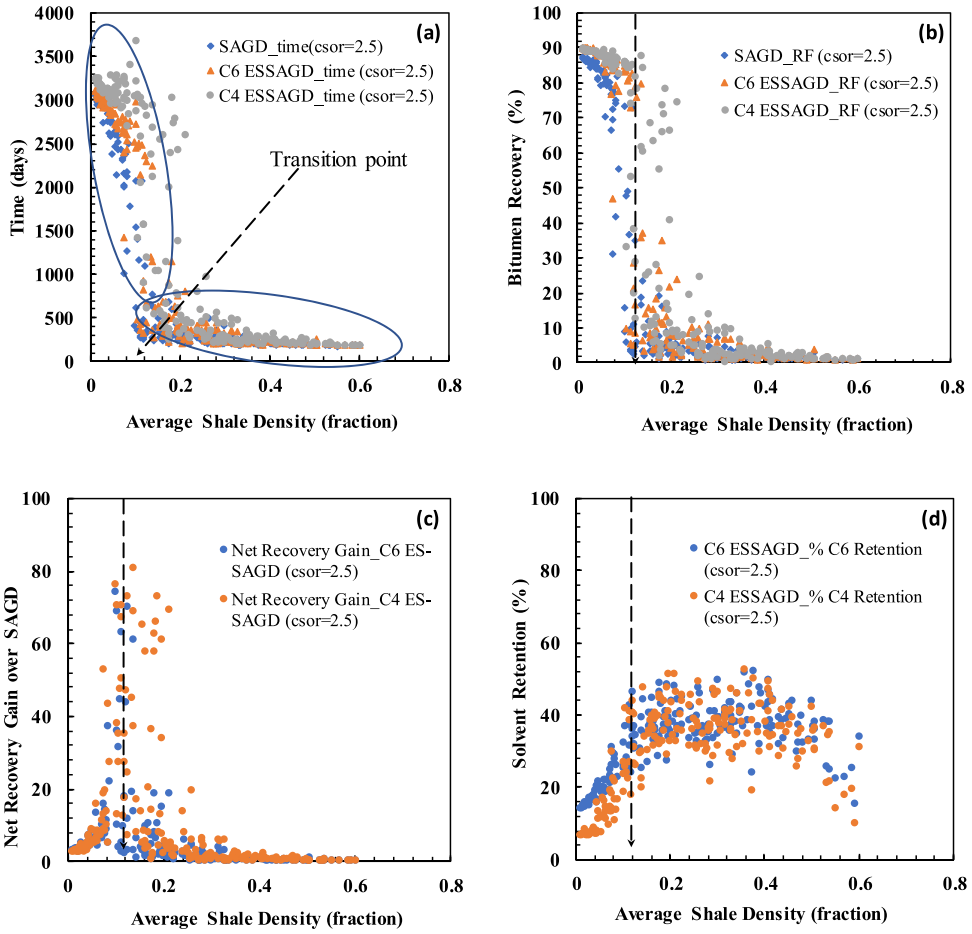

Figure 8. (a) Simulation time for cSOR = 2.5, (b) recovery (%) for cSOR = 2.5, (c) absolute recovery gain relative to SAGD for cSOR = 2.5, and (d) solvent retention (%) for cSOR = 2.5.

Table 2. Average of Simulation Results at cSOR = 2.5

	simulation time to reach cSOR = 2.5 (days)		bitumen recovery (%)		solvent retention (%)			
case	LSHD	HSHD	LSHD	HSHD	LSHD	HSHD	net/absolute recovery gain (%)	transition point shale density
SAGD	1580	219	47.0	2.0	NA	NA	NA	~0.12
C6 ES-SAGD	1919	246	57.5	3.0	27.0	38.2	5.7	
C4 ES-SAGD	2427	306	66.6	4.3	22.4	37.2	10.8	

An important point to note is the way the transition point behaves with the increasing cSOR. As we accommodate higher cut-offs of cSOR, higher shale fractions which are lower than the transition point value are also able to produce.

3.5. Cumulative SOR = 3.5. As we noticed during the previous cut-offs of cSOR, the transition points are shifting toward higher shale fractions. In other words, by allowing production till higher cSOR values, oil recovery from more heterogeneous shale barriers (higher shale fractions) can be improved. In our last analysis, we have chosen the maximum cSOR of 3.5. Total simulation time and bitumen recovery to reach a cSOR of 3.5 for both SAGD and ES-SAGD are plotted against shale density in Figure 10a,b. Figure 10c,d represents the average absolute gain in recovery and solvent retention for ES-SAGD cases, respectively.

From Table 4, we observed that the transition point is now close to what we have observed after a total simulation period of 20 years. This can be interpreted as if we produce more than this point of cSOR cut-off, there will not be any significant addition of bitumen recovery in shale fractions beyond this transition point. In other words, the transition point increases with the increasing cSOR cut-offs, but eventually plateaus. Comparing the results, both SAGD and ES-SAGD are able to recover more than 70% of bitumen, while ES-AGD is able to produce more than 80% in the LSHD region. The partition of LSHD and HSHD has been done at shale density = 0.2, which is the transition point.

Solvent retention is almost doubled in the HSHD region relative to the LSHD region for both the ES-SAGD cases. The average absolute gain in recovery at cSOR = 3.5 is very close to results obtained at cSOR = 3 for both C4 ES-SAGD and C6 ES-SAGD.

In Figure 11, we demonstrate the average absolute recovery gain for C6- and C4 ES-SAGD relative to SAGD for previously defined cSOR cut-offs. We observed, as explained in previous sections, that the rate of increase in absolute recovery gain

https://doi.org/10.1021/acsomega.2c02263
ACS Omega 2022, 7, 20280−20290

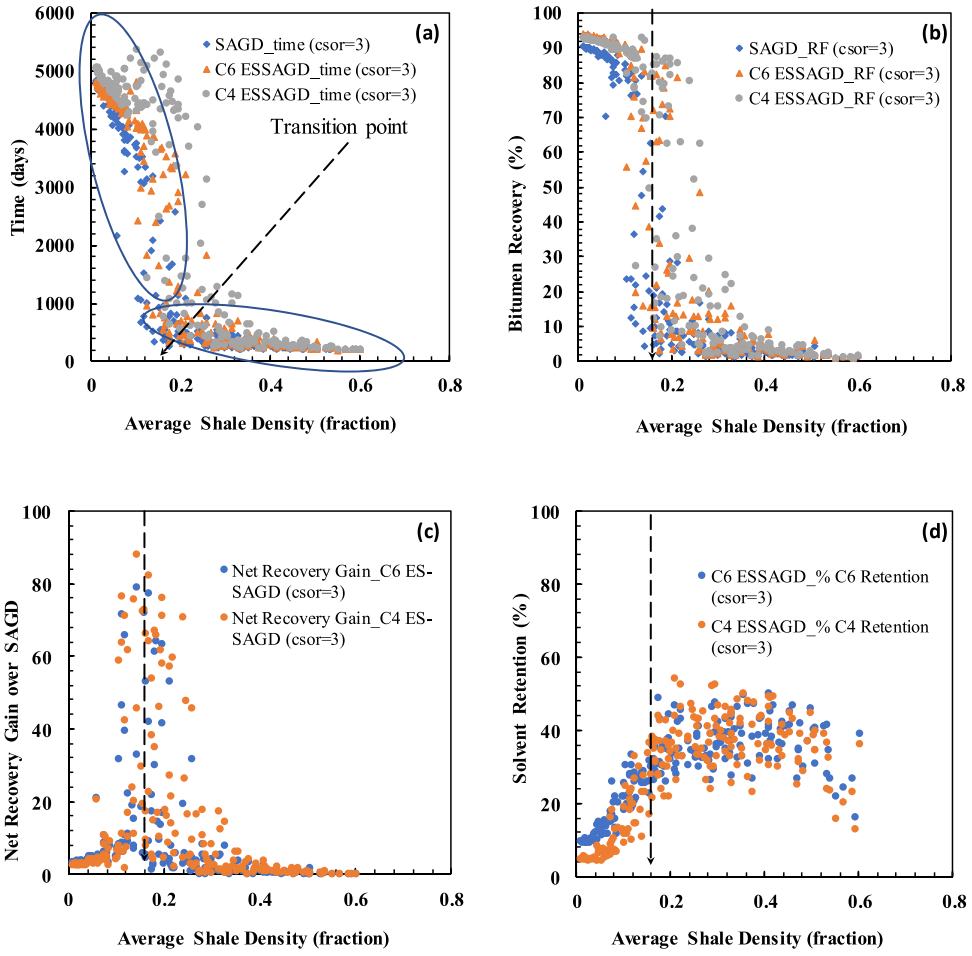

Figure 9. (a) Simulation time for cSOR = 3, (b) recovery (%) for cSOR = 3, (c) absolute recovery gain relative to SAGD for cSOR = 3, and (d) solvent retention (%) for cSOR = 3.

Table 3. Average of Simulation Results at cSOR = 3

case	simulation time to reach cSOR = 3 (days)		bitumen recovery (%)		solvent retention (%)			
	LSHD	HSHD	LSHD	HSHD	LSHD	HSHD	net/absolute recovery gain (%)	transition point shale density
SAGD	2908	287	61.3	3.4	NA	NA	NA	~0.16
C6 ES-SAGD	3580	383	75.3	6.0	20.7	36.9	8.2	
C4 ES-SAGD	4290	618	80.8	9.8	16.1	37.6	12.8	

increased at an almost constant rate for C4 ES-SAGD, excluding the highest cut-off of 3.5. For C6 ES-SAGD, the rate of increase is almost consistent from 2 to 3 but shows a slight decrease in the rate at 3.5.

4. CONCLUSIONS

This paper demonstrates an in-depth analysis of the impact of shale barriers in SAGD and ES-SAGD performance through multiple shale realizations. ES-SAGD has been analyzed by including a lighter (C4) and a heavier (C6) solvent. Multiple shale realizations (=216) covering a wide range of shale fraction/density have been used to generate a conclusive insight and trend in data obtained. Multiple cut-offs for cSOR are used to analyze the simulation results for SAGD and ES-SAGD. Following are the important conclusions drawn from the analysis performed in this paper:

- Incorporating more sensitivities based on different shale densities provides a greater insight into analyzing the impact of shale barriers on SAGD and ES-SAGD.
- ES-SAGD proves to be efficient in the presence of shale barriers relative to SAGD. Co-injection of C4 leads to better recovery than C6 in the presence of shale barriers.
- Transition points, defined as shale density at which the key performance measures (i.e., oil recovery, solvent retention), are used to group the shale density range into clusters showing a similar behavior.
- Due to delayed condensation of C4 relative to C6 and C4 in the vapor phase expands through the restricted paths in the presence of the shale barriers more easily. The C4 vapor phase propagation in tortuous pathways and its eventual condensation and dilution effect led to a better solvent performance, hence higher bitumen recovery in heterogeneous reservoirs.

https://doi.org/10.1021/acsomega.2c02263
ACS Omega 2022, 7, 20280−20290

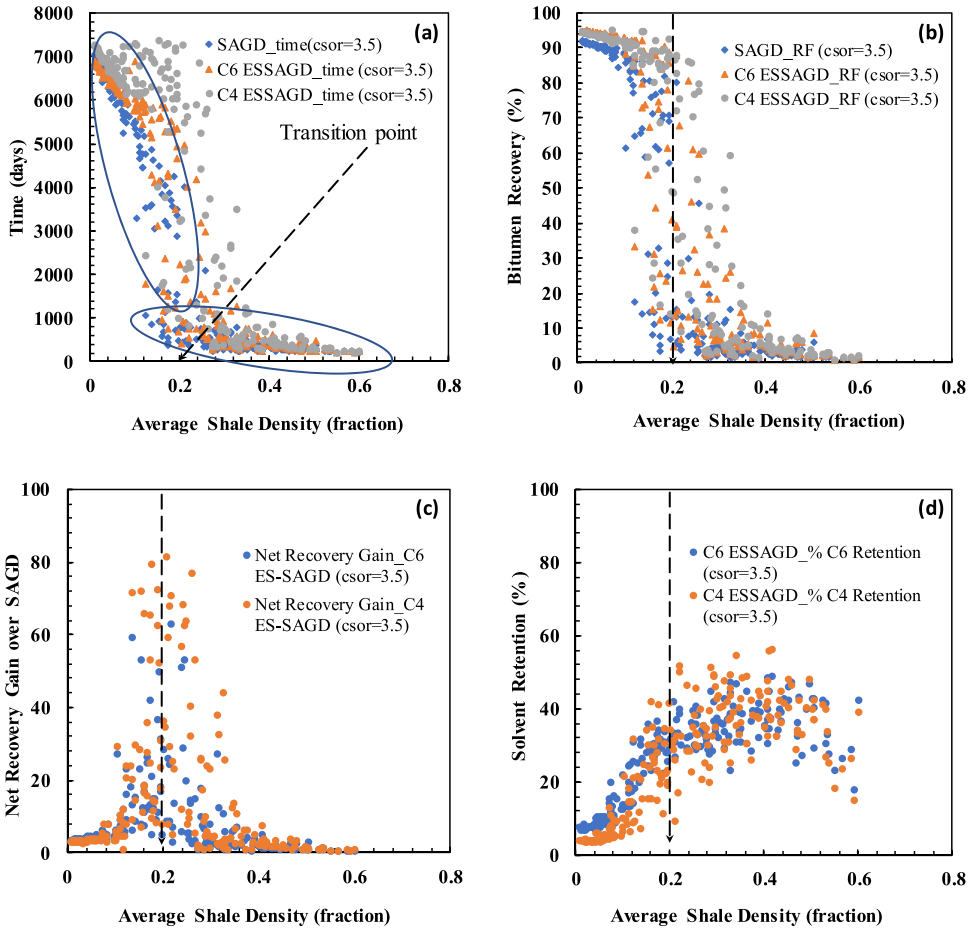

Figure 10. (a) Simulation time for cSOR = 3.5, (b) recovery (%) for cSOR = 3.5, (c) absolute recovery gain relative to SAGD for cSOR = 3.5, and (d) solvent retention (%) for cSOR = 3.5.

Table 4. Average of Simulation Results at cSOR = 3.5

case	simulation time to reach cSOR = 3.5 (days)		bitumen recovery (%)		solvent retention (%)		net/absolute recovery gain (%)	transition point shale density
	LSHD	HSHD	LSHD	HSHD	LSHD	HSHD		~0.2
SAGD	4808	424	74.0	5.9	NA	NA	NA	
C6 ES-SAGD	5541	708	83.6	11.5	16.5	35.3	7.6	
C4 ES-SAGD	6404	1323	86.9	18.5	12.1	36.4	12.8	

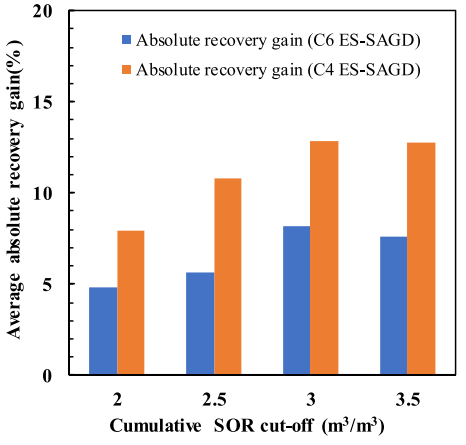

Figure 11. Absolute recovery gain for ES-SAGD over SAGD.

- Increasing the cut-off shifts the transition point value to higher shale densities, but it is found to be constant at cSOR cut-off higher than 3.5. From the analysis, these transition points in shale density were found to be highest for C4 ES-SAGD while lowest for SAGD, and C6 ES-SAGD values fall in the middle.
- Shale densities over 0.2 are detrimental to production. Although the recovery is increasing for ES-SAGD over SAGD; the absolute recovery (%) remains very low.
- Solvent retention is higher where shale density is greater than 0.2 relative to shale density less than 0.2 due to the presence of elongated continuous shales.
- A detailed economic analysis is required as future work for decision-making purposes.

https://doi.org/10.1021/acsomega.2c02263
ACS Omega 2022, 7, 20280−20290

AUTHOR INFORMATION

Corresponding Author

Hassan Hassanzadeh − *Department of Chemical & Petroleum Engineering, Schulich School of Engineering, University of Calgary, Calgary, Alberta T2N 1N4, Canada;* orcid.org/0000-0002-3029-6530; Email: hhassanz@ucalgary.ca

Author

Ashish Kumar − *Department of Chemical & Petroleum Engineering, Schulich School of Engineering, University of Calgary, Calgary, Alberta T2N 1N4, Canada*

Complete contact information is available at: https://pubs.acs.org/10.1021/acsomega.2c02263

Notes

The authors declare no competing financial interest.

ACKNOWLEDGMENTS

The authors acknowledge the financial support of the Natural Sciences and Engineering Research Council of Canada (NSERC) and all the member companies of the SHARP Research Consortium: Canadian Natural Resources Ltd., Cenovus Energy, CNOOC International, ConocoPhillips, Husky Energy, Imperial Oil Limited, Kuwait Oil Company, Osum Oil Sands, Strathcona Resources Ltd., and Suncor Energy. The support of the Department of Chemical and Petroleum Engineering and the Schulich School of Engineering at the University of Calgary is also acknowledged. Finally, Dr. Roger Butler Memorial Graduate Scholarship to Ashish Kumar is greatly acknowledged.

REFERENCES

(1) Dusseault, M. B. Comparing Venezuelan and Canadian heavy oil and tar sands. In *Canadian international petroleum conference*; Petroleum Society of Canada, 2001.

(2) Butler, R. M.; Stephens, D. J. The gravity drainage of steam-heated heavy oil to parallel horizontal wells. *J. Can. Pet. Technol.* **1981**, *20*, No. PETSOC-81-02-07.

(3) Nasr, T. N.; Beaulieu, G.; Golbeck, H.; Heck, G. Novel Expanding Solvent-SAGD Process "ES-SAGD". *J. Can. Pet. Technol.* **2003**, *42*, No. PETSOC-03-01-TN.

(4) Li, W.; Mamora, D. D.; Li, Y. Solvent-Type and -Ratio Impacts on Solvent-Aided SAGD Process. *SPE Res. Eval. Eng.* **2011**, *14*, 320−331.

(5) Redford, D. A.; McKay, A. S. Hydrocarbon-Steam Processes for Recovery of Bitumen from Oil Sands. In *Paper SPE 8823 presented at SPE/DOE Enhanced Oil Recovery Symposium*; OnePetro: Tulsa, Oklahoma, USA, 1980.

(6) Khaledi, R.; Boone, T. J.; Motahhari, H. R.; Subramanian, G. Optimized solvent for solvent assisted-steam assisted gravity drainage (SA-SAGD) recovery process. In *SPE Canada Heavy Oil Technical Conference*; Society of Petroleum Engineers, 2015.

(7) Sabet, N.; Hassanzadeh, H.; Abedi, J. Selection of efficient solvent in solvent-aided thermal recovery of bitumen. *Chem. Eng. Sci.* **2017**, *161*, 198−205.

(8) Nourozieh, H.; Kariznovi, M.; Abedi, J. Pentane as a Potential Candidate for ES-SAGD and Hybrid Processes: Its Phase Behaviour with Bitumen. In *SPE Heavy Oil Conference*; OnePetro, 2014.

(9) Zirrahi, M.; Hassanzadeh, H.; Abedi, J. Experimental measurements and correlation of K-value, viscosity, and density data for mixtures of light to heavy solvents and Athabasca bitumen with applications of ES-SAGD process. In *SPE Canada Heavy Oil Technical Conference*; OnePetro, 2016.

(10) Orr, B. ES-SAGD; past, present and future. In *SPE Annual Technical Conference and Exhibition*; Society of Petroleum Engineers, 2009.

(11) Yang, G.; Butler, R. M. Effects of reservoir heterogeneities on heavy oil recovery by steam-assisted gravity drainage. *J. Can. Pet. Technol.* **1992**, *31*, No. PETSOC-92-08-03.

(12) Yongrong, G.; Erpeng, G.; Jian, L.; Youwei, J.; Hongyuan, W.; Yao, W. Case Study on a New Approach for Exploiting Heavy Oil Reservoirs with Shale Barriers. In *SPE EOR Conference at Oil and Gas West Asia*; Society of Petroleum Engineers, 2016.

(13) Huang, S.; Yang, L.; Xia, Y.; Du, M.; Yang, Y. An experimental and numerical study of a steam chamber and production characteristics of SAGD considering multiple barrier layers. *J. Pet. Sci. Eng.* **2019**, *180*, 716−726.

(14) Kisman, K. E.; Yeung, K. C. Numerical study of the SAGD process in the Burnt Lake oil sands lease. In *SPE international heavy oil symposium*; Society of Petroleum Engineers, 1995.

(15) Pooladi-Darvish, M.; Mattar, L. SAGD operations in the presence of overlying gas cap and water layer-effect of shale layers. *J. Can. Pet. Technol.* **2002**, *41*, No. PETSOC-02-06-04.

(16) Chen, Q.; Gerritsen, M. G.; Kovscek, A. R. Effects of reservoir heterogeneities on the steam-assisted gravity-drainage process. *SPE Reservoir Eval. Eng.* **2008**, *11*, 921−932.

(17) Ipek, G.; Frauenfeld, T.; Yuan, J. Y. Numerical study of shale issues in SAGD. In *Canadian International Petroleum Conference*; Petroleum Society of Canada, 2008.

(18) Le Ravalec, M.; Morlot, C.; Marmier, R.; Foulon, D. Heterogeneity impact on SAGD process performance in mobile heavy oil reservoirs. *Oil Gas Sci. Technol.* **2009**, *64*, 469−476.

(19) Shin, H.; Choe, J. Shale barrier effects on the SAGD performance. In *SPE/EAGE reservoir characterization & simulation conference (pp. cp-170)*; European Association of Geoscientists & Engineers, 2009.

(20) Fatemi, S. M. The effect of geometrical properties of reservoir shale barriers on the performance of steam-assisted gravity drainage (SAGD). *Energy Sources, Part A* **2012**, *34*, 2178−2191.

(21) Dang, C. T. Q.; Chen, Z.; Nguyen, T. B. N.; Bae, W.; Mai, C. L. Numerical Simulation of SAGD Recovery Process in Presence of Shale Barriers, Thief Zones, and Fracture System. *Pet. Sci. Technol.* **2013**, *31*, 1454−1470.

(22) Wang, C.; Leung, J. Characterizing the effects of lean zones and shale distribution in steam-assisted-gravity-drainage recovery performance. *SPE Reservoir Eval. Eng.* **2015**, *18*, 329−345.

(23) Xia, Y.; Huang, S.; Chen, X.; Cao, M.; Yang, L. Study on the Characteristics of Production Performance and Steam Chamber of SAGD Considering Interlayer. In *SPE International Heavy Oil Conference and Exhibition*; Society of Petroleum Engineers, 2018.

(24) Zhang, L.; Li, J.; Sun, L.; Yang, F. An influence mechanism of shale barrier on heavy oil recovery using SAGD based on theoretical and numerical analysis. *Energy* **2020**, *216*, No. 119099.

(25) Kumar, A.; Hassanzadeh, H. Impact of shale barriers on performance of SAGD and ES-SAGD—A review. *Fuel* **2021**, *289*, No. 119850.

(26) Li, W.; Mamora, D.; Li, Y.; Qiu, F. Numerical investigation of potential injection strategies to reduce shale barrier impacts on SAGD process. *J. Can. Pet. Technol.* **2011**, *50*, 57−64.

(27) Ashrafi, M.; Souraki, Y.; Karimaie, H.; Torsaeter, O.; Kleppe, J. Numerical Simulation Study of SAGD Experiment and Investigating Possibility of Solvent Co-Injection. In *SPE Enhanced Oil Recovery Conference*; OnePetro, 2011.

(28) Venkatramani, A. V.; Okuno, R. Steam-Solvent Coinjection under Reservoir Heterogeneity: Should ES-SAGD be Implemented for Highly Heterogeneous Reservoirs?. In *SPE Canada Heavy Oil Technical Conference*; Society of Petroleum Engineers, 2017.

(29) Venkatramani, A. V.; Okuno, R. Mechanistic simulation study of expanding-solvent steam-assisted gravity drainage under reservoir heterogeneity. *J. Pet. Sci. Eng.* **2018**, *169*, 146−156.

(30) Kumar, A.; Hassanzadeh, H. A qualitative study of the impact of random shale barriers on SAGD performance using data analytics and machine learning. *J. Pet. Sci. Eng.* **2021**, *205*, No. 108950.

(31) CMG; *STARS: Users' Guide, Advanced Processes & Thermal Reservoir Simulator (Version 2018),* Computer Modeling Group: Calgary, AB, Canada, 2018.

(32) Haddadnia, A.; Sadeghi Yamchi, H.; Zirrahi, M.; Hassanzadeh, H.; Abedi, J. New solubility and viscosity measurements for methane−, ethane−, propane−, and butane−Athabasca bitumen systems at high temperatures up to 260° C. *J. Chem. Eng. Data* **2018**, *63*, 3566−3571.
(33) Haddadnia, A.; Zirrahi, M.; Hassanzadeh, H.; Abedi, J. Thermophysical properties of n-pentane/bitumen and n-hexane/bitumen mixture systems. *Can. J. Chem. Eng.* **2018**, *96*, 339−351.

https://doi.org/10.1021/acsomega.2c02263
ACS Omega 2022, 7, 20280−20290